Heterocycle-Substituted Stable Thioaminyl Radicals: Isolation, ESR Spectra, and Magnetic Properties[1]

Yozo Miura* and Tatsuya Tomimura

Department of Applied Chemistry, Faculty of Engineering, Osaka City University, Sumiyoshi-ku, Osaka 558-8585, Japan

Yoshio Teki

Department of Material Science, Graduate School of Science, Osaka City University, Sumiyoshi-ku, Osaka 558-8585, Japan

miura@a-chem.eng.osaka-cu.ac.jp

Received June 13, 2000

N-[(2-Benzothiazolyl)thio]- (**1**), *N*-[(2-benzoxazolyl)thio]- (**2**), and *N*-(2-pyrimidylthio)-2,4,6-trisubstituted-phenylaminyls (**3**) were generated by oxidation of the corresponding amines. Although **2** and **3** were not sufficiently persistent to be isolated, **1** was very persistent and could be isolated as radical crystals. The ESR spectra of nondeuterated and partially deuterated **1**−**3** radicals were measured, and the spin density distributions were estimated from the hyperfine coupling constants. Ab initio molecular orbital calculations were made for **1** to discuss the spin density distribution in more detail. Single-crystal X-ray crystallographic analysis was performed for one radical. Magnetic properties were measured for isolated four radicals with a SQUID. Two radicals showed ferromagnetic interaction, and analyses of χT vs T plots with the one-dimensional regular Heisenberg model gave $2J/k_B = 5.8$ and 8.6 K. The remaining two radicals showed antiferromagnetic interaction. Analyses of the χT vs T plots with the Curie−Weiss law or dimer model gave $\theta = -1.4$ K and $2J/k_B = -1370$ K. The strong antiferromagnetic interaction could be explained in terms of the X-ray crystallographic results.

Introduction

Thioaminyl radicals are interesting not only as a family of oxygen-insensitive isolable radicals but also as challenging targets for molecule-based magnets.[2,3] Recently, the −N̈−S− containing cyclic radicals showed interesting magnetic[4,5] and concucting properties.[6] Since thioaminyl radicals have an extensively delocalized π-spin system, their magnetic interactions in solids are expected to be strong. Furthermore, this new spin system is useful as building blocks for new functionalized magnetic materials.[7] In our studies on thioaminyls[2,3] we studied the magnetic properties of the isolated radical crystals with a SQUID. The magnetic results have showed that they have strong intermolecular interactions in solids, compared with nitroxides or nitronyl nitroxides having the localized unpaired electron spin.[8] For example, the intrachain ferromagnetic interactions ($2J/k_B$) observed for *N*-[(2,4-dichlorophenyl)thio]-2,4,6-tris(4-chlorophenyl)-phenylaminyl,[9] *N*-[(4-nitrophenyl)thio]-4-ethoxycarbonyl-2,6-bis(4-chlorophenyl)phenylaminyl,[10] and *N*-[(2,4-dichlorophenyl)thio]-4-phenyl-2,6-bis(3-pyridyl)phenylaminyl[1] are 28.0, 16.0, and 22.4 K, respectively, which are much larger than those of organic free radicals so far reported.[11] However, a severe problem is that the desired thioaminyl radicals cannot always be isolated. We have so far designed many structurally interesting thioaminyls and examined possibilities of isolation. Although in some cases isolation of radicals was successful, we have also encountered many unsuccessful cases. In the present studies three types of heterocycle-substituted thioaminyls, *N*-[(2-benzothiazolyl)thio]- (**1**), *N*-[(2-benzoxazolyl)-thio]- (**2**), and *N*-(2-pyrimidylthio)-2,4,6-trisubstituted-phenylaminyls (**3**) (Chart 1), were prepared and their stabilities examined. Since benzothiazole, benzoxazole, and pyrimidine rings are interesting π-electron systems, 1−3 may be expected to show interesting magnetic

(1) ESR Studies of Nitrogen-Centered Free Radicals. 52. For part 51, see: Miura, Y.; Kurokawa, S.; Nakatsuji, M.; Ando, K.; Teki, Y. *J. Org. Chem.* **1998**, *63*, 8295−8303.

(2) Miura, Y. *Trends Org. Chem.* **1997**, *6*, 197−217.

(3) Miura, Y. *Recent Res. Dev. Org. Chem.* **1998**, *2*, 251−268.

(4) Banister, A. J.; Bricklebank, N.; Lavender, I.; Rawson, J. M.; Gregory, C. I.; Tanner, B. K.; Clegg, W.; Elsegood, M. R. J.; Palacio, F. *Angew. Chem., Int. Ed. Engl.* **1996**, *35*, 2533−2535.

(5) Fujita, W.; Awaga, K. *Science*, **1999**, *286*, 261−262.

(6) Barclay, T. M.; Cordes, A. W.; Haddon, R. C.; Itkis, M. E.; Oakley, R. T.; Reed, R. W.; Zhang, H. *J. Am. Chem. Soc.* **1999**, *121*, 969. Barclay, T. M.; Cordes, A. W.; Oakley, R. T.; Preuss, K. E.; Reed, R. W. *Chem. Mater.* **1999**, *11*, 164. Barclay, T. M.; Beer, L.; Cordes, A. W.; Oaklay, R. T.; Preuss, K. E.; Taylor, N. J.; Reed, R. W. *J. Chem. Soc., Chem. Commun.* **1999**, 531. Barclay, T. M.; Beer, L.; Cordes, A. W.; Haddon, R. C.; Itkis, M. I.; Oakley, R. T.; Preuss, K. E.; Reed, R. W. *J. Am. Chem. Soc.* **1999**, *121*, 6657. Barclay, T. M.; Cordes, A. W.; George, N. A.; Haddon, R. C.; Itkis, M. E.; Oakley, R. T. *J. Chem. Soc., Chem. Commun.* **1999**, 2269. Chi, X.; Itkis, M. E.; Patrick, B. O.; Barclay, T. M.; Reed, R. W.; Oakley, R. T.; Cordes, A. W.; Haddon, R. C. *J. Am. Chem. Soc.* **1999**, *121* 10395.

(7) Kaszynski, P. In *Magnetic Properties of Organic* Materials; Lahti, P. M., Ed.; Marcel Dekker: New York and Basel, 1999; Chaper 15.

(8) (a) Forrester, A. R.; Hay, J. M.; Thomson, R. H. *Organic Chemistry of Stable Free Radicals*; Academic Press: London and New York, 1968. (b) Rozantsev, E. G. *Free Nitroxide Radicals*; Plenum Press: New York and London, 1970. (c) Volodarsky, L. B.; Reznikov, V. A.; Ovcharenko, V. I. *Synthetic Chemistry of Stable Nitroxides*; CRC Press: Boca Raton, FL, 1994.

(9) Teki, Y.; Itoh, K.; Okada, A.; Yamakage, H.; Kobayashi, T.; Amaya, K.; Kurokawa, S.; Ueno, S.; Miura, Y. *Chem. Phys. Lett.* **1997**, *270*, 573−579.

(10) Miura, Y. Momoki, M.; Nakatsuji, M.; Teki, Y. *J. Org. Chem.* **1998**, *63*, 1555−1565.

(11) (a) *Magnetic Properties of Organic* Materials; Lahti, P. M., Ed.; Marcel Dekker: New York and Basel, 1999. (b) Proceedings of the Fifth International Conference on Molecule-Based Magnets; Kahn, O., Ed.: *Mol. Cryst. Liq. Cryst.* **1999**, *334*, 1−712; *335*, 1−706.

10.1021/jo000901q CCC: $19.00
Published on Web 10/21/2000

Chart 1

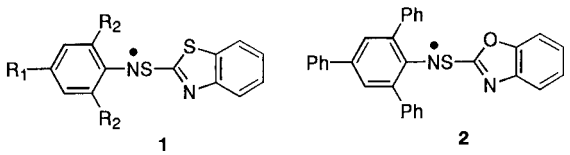

1 **2**

a: $R_1 = R_2 =$ Ph
b: $R_1 = R_2 =$ 4-ClC_6H_4
c: R_1 = MeCO, R_2 = Ph
d: R_1 = EtOCO, R_2 = 4-ClC_6H_4

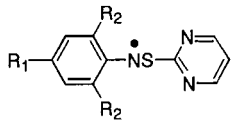

3

a: R_1 = Ph
b: R_1 = 4-ClC_6H_4

Scheme 1

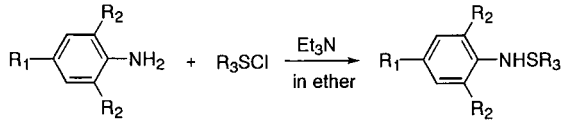

4-6

4a: $R_1 = R_2$ = Ph, R_3 = 2-benzothiazolyl
4b: $R_1 = R_2$ = 4-ClC_6H_4, R_3 = 2-benzothiazolyl
4c: R_1 = MeCO, R_2 = Ph, R_3 = 2-benzothiazolyl
4d: R_1 = EtOCO, R_2 = 4-ClC_6H_4, R_3 = 2-benzothiazolyl
5: $R_1 = R_2$ = Ph, R_3 = 2-benzoxazolyl
6a: $R_1 = R_2$ = Ph, R_3 = 2-pyrimidyl
6b: $R_1 = R_2$ = 4-ClC_6H_4, R_3 = 2-pyrimidyl

properties. Among the three heterocycle-substituted thioaminyl radicals examined, **1** was very persistent and could be isolated as radical crystals. On the other hand, the other two radicals were not sufficiently persistent to be isolated. In the present paper we report isolation, ESR spectra, single-crystal X-ray analysis, ab initio molecular orbital calculations, and magnetic properties of **1**, along with ESR spectra of **2** and **3**.

Results and Discussion

Preparation of Radical Precursors. The corresponding precursors of radicals, **4**−**6**, were prepared according to Scheme 1. Compounds **4** were prepared by the reaction of 2,4,6-trisubstituted anilines with 2-benzothiazolesulfenyl chloride. As the sulfenyl chloride was added to a solution of a trisubstituted aniline, the reaction mixture showed an intense green or blue color, indicating that a considerable amount of **1** was formed in the reaction mixture. After filtration, TLC analysis showed that the starting aniline almost completely disappeared and **4** was formed in a high yield, along with formation of a considerable amount of **1**. The bis(2-benzothiazolyl) disulfide formed was readily removed due to the poor solubility in ordinary organic solvents. When column chromatography of the reaction mixture was conducted at room temperature, complete decomposition of **4** was observed. Accordingly, it was carried out at 0 °C using a short column to remove the starting aniline and a less polar byproduct. After column chromatography and subsequent concentration, crystallization of the residue (amorphous) was attempted using a variety of solvents, but it was always unsuccessful, giving only an amorphous material. We therefore used the raw products in the next oxidation step without further purification. Fortunately, due to the good crystallinity of **1** their isolation was successful, though the yields were very low (11−22%).

Precursor 5 was prepared by the reaction of trisubstituted anilines with 2-benzoxazolesulfenyl chloride. Different from the case of **4**, the reaction mixture turned orange upon addition of the sulfenyl chloride, and appearance of an intense green or blue color attributable to **2** was not observed. TLC analysis of the reaction mixture showed that it was a ca. 1:1 mixture of **5** and the starting aniline containing a small amount of a less polar byproduct[12] After column chromatography at 0 °C using a short column, crystallization of the mixture of **5** and the starting aniline was attempted, but no crystals were obtained. For generation of **2**, the mixture was used without further purification.

Precursors **6** were prepared by the reaction of trisubstituted anilines with 2-pyrimidinesulfenyl chloride. In this case the mixture turned light green upon addition of the sulfenyl chloride, and TLC analysis of the reaction mixture indicated complete disappearance of the starting aniline and a high-yield formation of **6**. Upon column chromatography at 0 °C using a short column, almost pure **6** was obtained and recrystallization from hexanes−ethyl acetate gave colorless prisms in 43−65% yields. The structures of **6** were confirmed by ^{1}H NMR spectra and elemental analyses.

Generation and Isolation of Radicals. Radicals **1**−**3** were generated by oxidation of precursors **4**−**6** with PbO_2 under atmospheric conditions. Upon addition of PbO_2 to stirred solutions of precursors, dark green (**4a**−**c**, **5**, **6a**,**b**) or dark blue (**4d**) solutions were obtained, and intense ESR signals were observed for all solutions. Although in the oxidation of **4** and **5** the corresponding precursors almost completely disappeared, in the case of **6** significant amounts of precursors were shown to remain unreacted by TLC. This low reactivity of **6** for oxidation can be attributed to the presence of the strong electron-withdrawing pyrimidine group which makes the NH oxidation more difficult.

Interestingly, a solution of **1** kept the intense green or blue color constant for a long time, and this observation prompted us to isolate radicals of **1**. On the other hand, solutions of **2** and **3** could not keep the characteristic color over a long time. When the samples were standing for 1 day, the characteristic color almost completely disappeared. A brief kinetic study using ESR showed the half-life times of **2** and **3** in benzene at 20 °C (in the presence of atmospheric oxygen) were ca. 7 and 2 h, respectively. The reason only **1** is quite persistent and the other two radicals are not sufficiently persistent to be isolated is unclear at the present time.

Oxidation of **4** with PbO_2 in benzene, removal of the solvent by freeze-drying, and crystallization of the residue from hexanes−ethyl acetate (**1a**,**b**,**d**) or ethanol (**1c**) gave dark blue or dark green radical crystals in 11−22% yields. The spin concentrations of the isolated radicals determined by ESR were >93% for **1a**−**c** and 87% for **1d**. Although, since the spin concentration of **1d** was

(12) Bis(2-benzoxazolyl) disulfide was readily removed by filtration, similar to bis((2-benzothiazolyl) disulfide, because of the poor solubility in ordinary oragnic solvents.

Table 1. Hyperfine Coupling Constants and *g* Values for 1−3 in Benzene at 20 °C[a]

radical	a_N[b]	a_{other}[c]	g
1a	0.905		2.0051
1b	0.898		2.0052
1c[d]	0.883	0.151 (2 H),[e] 0.095 (1 N)[f]	2.0057
1d[d]	0.903	0.153 (2 H),[e] 0.098 (1 N)[f]	2.0056
1a-*d*[d]	0.907	0.144 (2 H),[e] 0.082 (1 N),[f] 0.37 (^{33}S)[g,h]	2.0051
2	0.897		2.0050
2-*d*[d]	0.903	0.140 (2 H),[e] 0.068 (1 N)[i]	2.0051
3a	0.906		2.0052
3b	0.901		2.0055
3a-*d*[d]	0.906	0.138 (2 H)[e]	2.0052
7[j]	0.894	0.133 (2 H)[e], 0.51 (^{33}S)	2.0059

[a] The hyperfine coupling (hfc) constants are given in mT. [b] The hfc constant for the NS nitrogen. [c] The numbers in parentheses refer to the number of equivalent protons or nitrogens. [d] The hfc constants are determined by computer simulation. [e] The hfc constants for the anilino meta protons. [f] The hfc constant for the benzothiazole nitrogen. [g] The value for ^{33}S at natural abundance. [h] The hfc constant for the NS sulfur. [i] The hfc constant for the benzoxazole nitrogen. [j] Taken from ref 13.

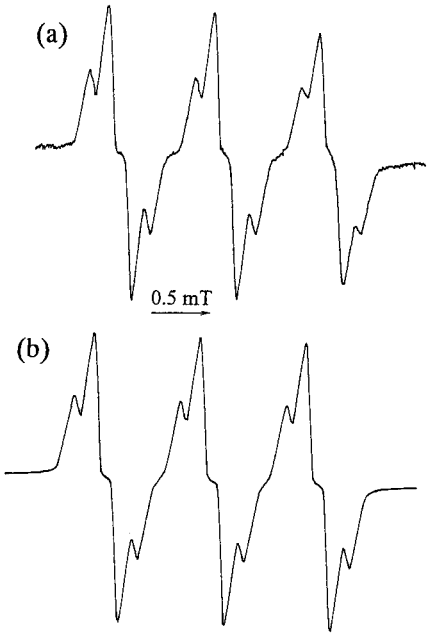

Figure 1. ESR spectrum of **1c** in benzene at 20 °C: (a) observed ESR spectrum; (b) computer simulation.

unsatisfactory, recrystallizations were repeated using a variety of solvents, no significant increase in the spin concentration was observed.

ESR Spectra of Radicals. ESR spectra of **1**−**3** were measured at room temperature using benzene as the solvent. The ESR parameters are summarized in Table 1, and a typical ESR spectrum is shown in Figure 1. Thioaminyls **1a**,**b**, **2**, and **3** gave a spectrum consisting of a broad 1:1:1 triplet, and no hyperfine couplings (hfc's) due to aromatic protons were observed. On the other hand, in the cases of **1c**,**d** each component of the 1:1:1 triplet was further split into an incomplete 1:3:3:1 quartet (see: Figure 1). Computer simulation of the spectra of **1c**,**d** gave a_N = 0.883 and 0.098 and a_H = 0.151 mT (2 H) (**1c**) and a_N = 0.903 and 0.107 and a_H = 0.153 mT (2 H) (**1d**). Upon deuteration of the three substituted phenyl groups of **1a**, **2**, and **3a,** the ESR spectra reduced significantly the line width to give relatively well-resolved hyperfine splittings (Figure 2). In the case of **1a**-*d* and **2**-*d* (Chart 2), each component of the 1:1:1 triplet was

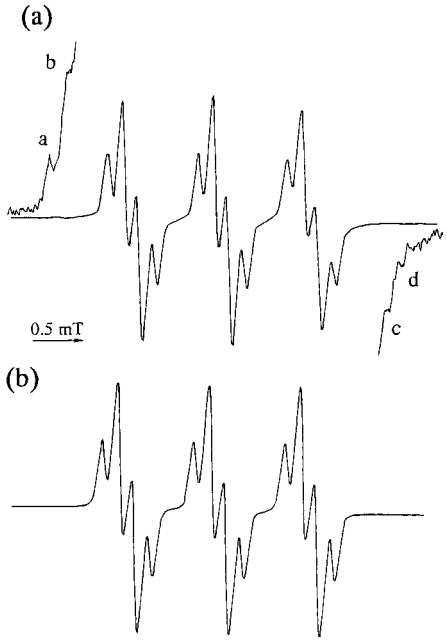

Figure 2. ESR spectrum of **1a**-*d* in benzene at 20 °C: (a) observed ESR spectrum; (b) computer simulation. In (a) both wings are recorded at high gain (100 times) and satellite lines due to ^{33}S at natural abundance (0.76%) are observed: a and b, $M_N = +1$, $M_S = +3/2$; c and d, $M_N = -1$, $M_S = -3/2$.

Chart 2

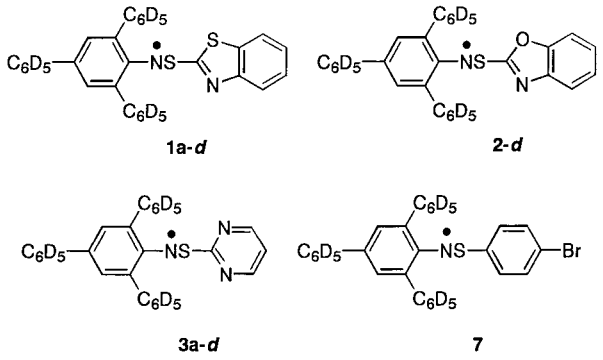

further split into a 1:3:3:1 quartet, similar to **1c**,**d**, as shown in Figure 2. However, the resolution of the spectra was improved, allowing more reliable computer analyses of the ESR spectra. In the case of **3a**-*d* the ESR spectrum was split into a 1:1:1 triplet of 1:2:1 triplets. Different from the spectra of **1a**-*d* and **2**-*d*, the hyperfine splittings due to the heterocyclic nitrogens were not observed. Computer simulation gave a_N = 0.906 and a_H = 0.138 mT (2 H).

The nitrogens giving a_N of 0.883−0.907 mT are obviously due to the central nitrogen, and the two equivalent protons with a_H of 0.138−0.153 mT are assigned to the anilino meta protons, in analogy with radicals **7**[13](see Table 1). On the other hand, the nitrogens with the hfc constants of 0.068−0.098 mT are assigned to the benzothiazole or benzoxazole nitrogen. These assignments were supported by ab intio molecular orbital (MO) calculations described below.

When both wings of the ESR spectrum of **1a**-*d* were recorded at high gain (100 times the parent spectrum),

(13) Miura, Y.; Tanaka, A.; Hirotsu, K. *J. Org. Chem.* **1991**, *56*, 6638−6643.

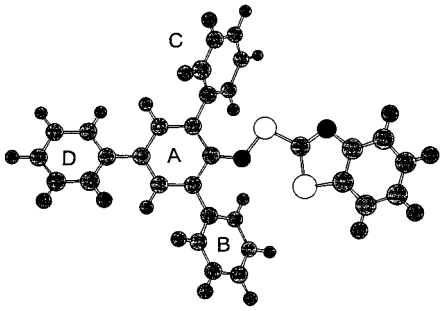

Figure 3. Optimized structure of 1a by the semiempirical MO calculations (MNDO/AM1 method).

Scheme 2

satellite lines due to ^{33}S at natural abundance (0.76%) could be observed, as found in Figure 2. From the figure a^{33}_S was determined to be 0.37 mT. The assignment of the satellite lines due to ^{33}S was made by the intensity ratio of the satellite lines to the parent spectrum. The intensity observed is 0.25%, which is in good agreement with the theoretical value (0.19%).

The hfc constants obtained for **1**−**3** were compared with those for the structurally related thioaminyls previously studied. Since the structure of **1a** (and **1a**-*d*) is similar to that of **7**, they are compared to each other. While the a_N (0.905−0.907 mT) and a_H values (0.151 mT) for **1a** and **1a**-*d* are somewhat larger than those (a_N = 0.894 mT, a_H = 0.133 mT) of **7**, the a^{33}_S (0.37 mT) is considerably smaller than that (0.51 mT) of **7**. Thioaminyl radicals are represented by two typical canonical structures A and B in which the unpaired electron is accommodated in the antibonding orbital (Scheme 2). The presence of an electron-withdrawing group at the S-side enhances the relative importance of canonical structure A (and reduces the relative importance of canonical structure B). In this view, the presence of an electron-withdrawing benzothiazole group at the S-side reduces the relative importance of canonical structure B, and this leads an reduction of a^{33}_S, along with an increase in a_N for the central N.

Spin Density Calculations. To discuss the spin density distribution in more detail, ab initio MO calculations based on the density functional theory were carried out for **1a**. The electronic structure of the molecule was calculated using Gaussian 98, and the molecular structure was optimized by the semiempirical MO calculations (MNDO/AM1 method). In the ab initio calculations, the STO 6-31G basis set and UHF Becke 3LYP hybrid method were employed.

The optimized structure of **1a** is shown in Figure 3, which is very similar to that determined by the X-ray crystallographic analysis performed for **1c** described below. This is shown by the excellent agreements of the bond lengths, bond angles, and torsion angles between the calculations and the observations as follows [calcd values (obsd values)]: C1−N1, 1.335 Å (1.372 Å); N1−S1, 1.625 Å (1.623 Å); S1−C19, 1.701 Å (1.732 Å); C1−N1−S1, 123.5° (122.0°); N1−S1−C19, 102.8° (99.0°); C2−C1−N1−S1, −172.9° (168.2°); C1−N1−S1−C19, 173.2° (173.4°); N1−S1−C19−N2, 172.5° (−172.8°). On the other hand, somewhat large deviations are observed for the dihedral angles between the A (C1−C6) and B (C7−C12) benzene rings and between the A and C (C13−C18) benzene rings. The calculated values are 46.6 and 59.8°, respectively, while the observed values are 54.2 and 77.0°.

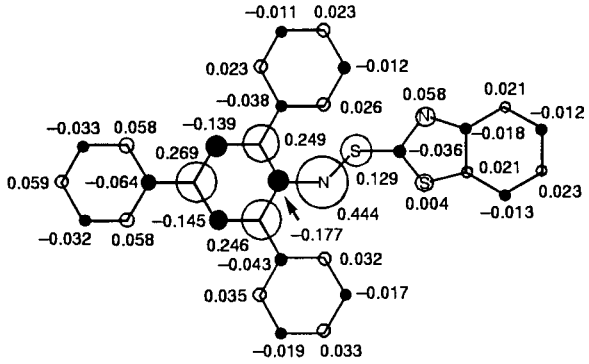

Figure 4. Total atomic spin densitiies for **1a** calculated by the ab initio MO calculations (Gaussian 98) using the STO 6-31G basis set and UHF Becke 3LYP hybrid method.

Table 2. Calculated Hfc Constants of 1a

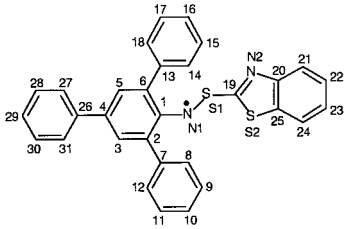

posn	calcd hfc const[a,b]	obsd hfc const[b−d]
3[e]	0.262	0.144
5[e]	0.268	0.144
N1	1.070	0.907
S1	0.299	0.37
N2	0.124	0.082

[a] The hfc constants were calculated by the ab initio MO method (Gaussian 98) using the STO 6-31G basis set and UHF Becke 3LYP hybrid method. [b] The hfc constants are given in mT. [c] The values for **1a**-*d* are shown. [d] The hfc constants are shown in the absolute values. [e] The hfc constants for the attached protons are shown.

The total atomic spin densities on the carbons, nitrogens, and sulfurs are shown in Figure 4, and some calculated hfc constants for the nitrogens, sulfurs, and protons are shown in Table 2. Although the calculated a_N and a_H values are somewhat larger than the experimental values and the calculated a^{33}_S value is smaller, satisfactory agreements between the calculations and experimentals are observed. On the basis of the ab initio MO calculations, we can estimate exactly the spin density distribution in **1**. As expected, the unpaired electron spin densities are high on the NS nitrogen and sulfur and the anilino benzene ring. A small delocalization of the unpaired electron spin onto the benzothiazole ring is observed. Although delocalization of the unpaired electron spin onto the three substituted benzene rings is small or negligibly small, the largest delocalization is observed for the D benzene ring (C26−C31) because the twisted angle is smallest (31.9°). On the other hand, the delocalization onto the B and C benzene rings is negligibly small due to the large twisted angles.

Single-Crystal X-ray Analysis. Since radical **1c** gave single crystals suitable for X-ray crystallographic analy-

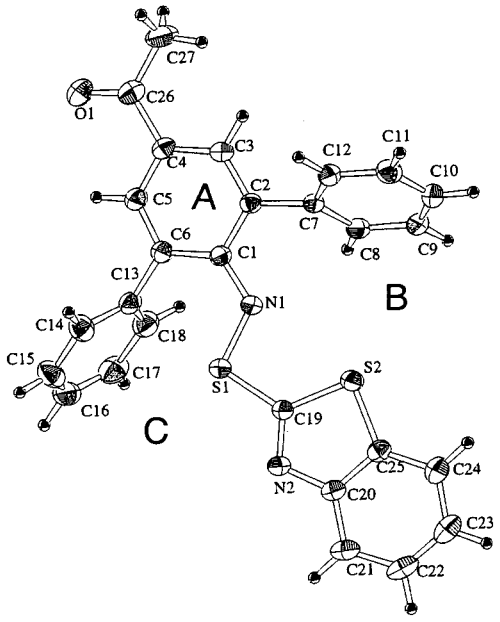

Figure 5. ORTEP drawing of **1c**.

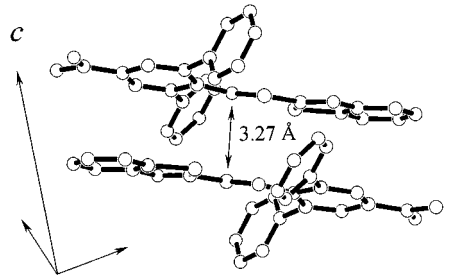

Figure 6. Crystal structure of **1c**. Only one dimer is described for clarity.

sis, we could perform the X-ray analysis for the radical. An ORTEP drawing and crystal structure are shown in Figures 5 and 6, respectively, and selected bond lengths, bond angles, and torsion angles are summarized in Table 3.

The ORTEP drawing shows that the dihedral angle between the A benzene ring and benzothiazole ring is 9.7° and the torsion angles for C1−N1−S1−C19, S1−N1−C1−C2, and N1−S1−C19−S2 are 173.4(3), 168.2(2), and 7.1(2)°, respectively, indicating that the A benzene ring, the N and S atoms, and the benzothiazole ring are approximately planar. It is therefore well explained that an extensive delocalization of the unpaired electron onto both the anilino benzene ring and the benzothiazole ring is possible, in accordance with the ESR results desribed above. The dihedral angles between the A and B benzene rings and between the A and C benzene rings are 54.2 and 77.0°, respectively, indicating that delocalization of the unpaired electron spin onto the B and C benzene rings is very small or negiligibly small. The large twisting of the C benzene ring from the A benzene ring is suggestive of a larger steric repulsion between the C benzene ring and the S atom.

The N−S bond length is 1.623 Å, which is significantly shorter than expected for the N−S single bond (1.694 Å).[14] This can be explained in terms of the three-electron bond between the nitrogen and sulfur.[15] The C1−C2 and C1−C6 double bonds are 1.428(5) and 1.444(4) Å, which are much longer than the usual C−C double bond of the

Table 3. Selected Bond Lengths and Angles and Torsion Angles for 1c

Bond Lengths (Å)	
C1−N1	1.372(4)
N1−S1	1.623(3)
S1−C19	1.732(3)
C1−C2	1.428(5)
C1−C6	1.444(4)
Bond Angles (deg)	
C1−N1−S1	122.0(2)
N1−S1−C19	99.0(2)
C2−C1−N1	115.0(3)
C6−C1−N1	126.9(3)
S1−C19−S2	122.9(2)
S1−C19−N2	119.6(2)
Torsion Angles (deg)	
S1−N1−C1−C2	168.2(2)
S1−N1−C1−C6	−11.7(5)
C1−N1−S1−C19	173.4(3)
S2−C19−S1−N1	7.1(2)
N2−C19−S1−N1	−172.8(3)

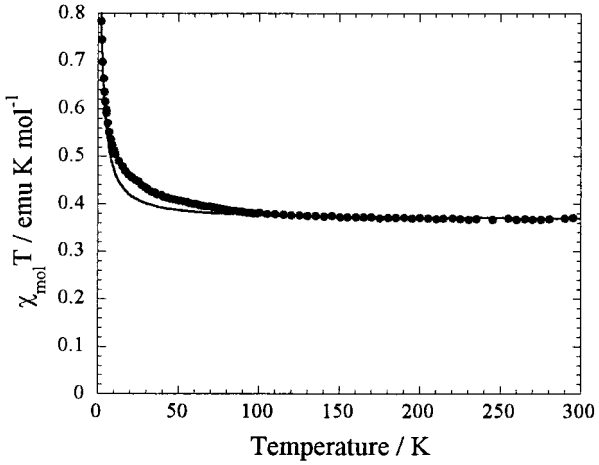

Figure 7. χT vs T plots of **1b**. The solid curve represents theoretical susceptibilities calculated with the one-dimensional regular Heisenberg model with $2J/k_B = 5.8$ K.

Chart 3

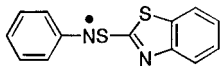

8

benzene ring (ca 1.38−1.40 Å).[16] Although the unusual long bond lengths may be explained by steric congestion around the radical center, the MNOD/AM1 calculations for **8** (Chart 3), which has no significant steric congestion around the nitrogen,[17] gave similar long bond lengths (1.440 Å) for the C1−C2 and C1−C6 bonds (the calculations of **1a** gave 1.463 and 1.454 Å for the bonds, respectively). Therefore, the long bond lengths may be explained in terms of the unique electronic structure of **1** in which the unpaired electron is accommodated in the antibonding orbital,[15] but the clear reasons are not obtained at the present time.

(14) Miura, Y.; Yamamoto, A.; Katsura, Y.; Kinoshita, M.; Sato, S.; Tamura, C. *J. Org. Chem.* **1982**, *47*, 2618−2622.
(15) Baird, N. C. *J. Chem. Educ.* **1977**, *54*, 291.
(16) Allen, F. H.; Kennard, O.; Watson, D. G.; Brammer, L.; Orpen, A. G. Taylor, R. *J. Chem. Soc., Perkin Trans. 2* **1987**, S1.
(17) The optimized structure of **8** was calculated by the semiempirical MO calculations (MNDO/AM1 method), similar to the calculations for **1a**.

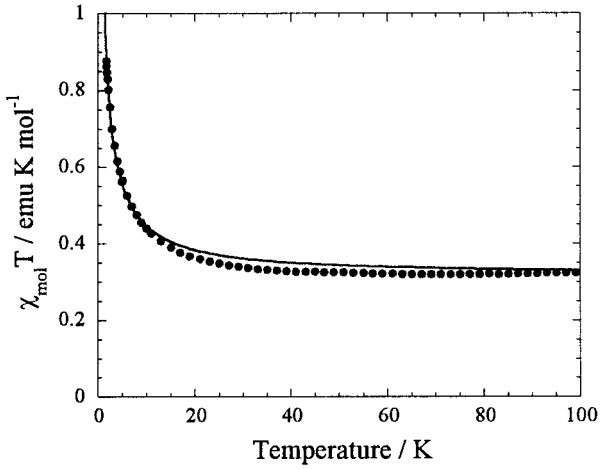

Figure 8. χT vs T plots of **1d**. The solid curve represents theoretical susceptibilities calculated with the one-dimensional regular Heisenberg model with $2J/k_B = 8.6$ K.

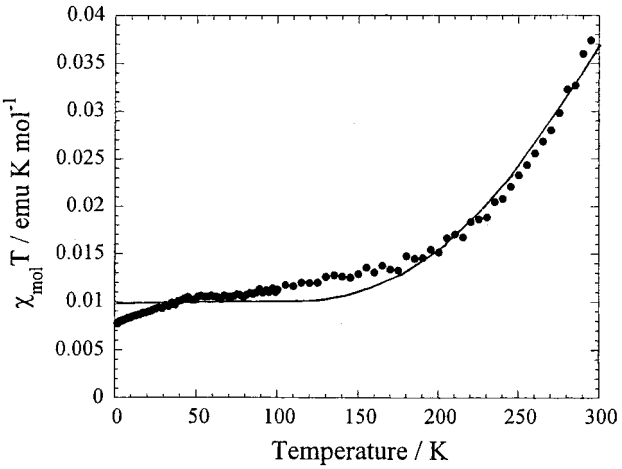

Figure 9. χT vs T plots of **1c**. The solid curve represents theoretical susceptibilities calculated with the dimer model with $2J/k_B = -1360$ K.

Magnetic Properties of Isolated Radicals. The magnetic properties of the isolated four radicals were measured on a SQUID using polycrystalline samples in the temperature range 1.8−300 K. The diamagnetic contribution was estimated using Pascal's constants.

The χT vs T plots for **1b** are shown in Figure 7. The χT values are constant in the temperature range 50−300 K, and from the χT value (0.364 emu K mol^{-1}) the spin concentration was determined to be 97%. On the other hand, below 50 K the χT value is increased with decreasing temperature, indicating that intermolecular interaction is ferromagnetic. Analysis of the χT vs T plots with the one-dimensional regular Heisenberg model [18] (eq 1) gave $2J/k_B = 5.8$ K. Radical **1d** also showed ferromagnetic interaction, as found in Figure 8. The spin concentration of this radical determined with a SQUID was 86%, which agreed with that (87%) determined by ESR. Analysis of the χT vs T plots using the one-dimensional regular Heisenberg model gave $2J/k_B = 8.6$ K. Since the spin concentration is not high, the value may contain a small error from the collected one.

$$H = -2J\Sigma S_i S_j \qquad (1)$$

Radicals **1a**,**c** showed antiferromagnetic interaction. Since in the case of **1a** the interaction was very weak, analysis of the experimental data was performed using the Curie−Weiss law to give −1.4 K as θ. The χT vs T plots of **1c** are shown in Figure 9. At room temperature, the χT value is already much lower than the theoretical value (0.375 emu K mol^{-1} of the Curie constant for 1/2 spin systems), and it was further decreased with decreasing temperature, indicating that a strong antiferromagnetic interaction operates between the radical molecules. Analysis of the χT vs T plots with the dimer model gave $2J/k_B = -1360$ K. This unusually strong antiferromagnetic interaction is well explained by the crystal structure. Figure 6 shows that radical molecules form a radical pair in which they are related by a center of inversion, and the dimers are arranged along the c axis in a zigzag manner. Within the dimer the shortest intermolecular distances are 3.27 Å (N1···S1') and 3.55 Å (N1···N1'). Since the spin densities on the NS nitrogen and sulfur are very high (the calculations show 0.444 and 0.129 on the NS nitrogen and sulfur, respectively), the unusually strong antiferromagnetic interaction can be well explained by this crystal structure. On the other hand, the nearest distances between the dimers were too long to interact with one another.

Conclusions

Three kinds of heterocycle-bearing thioaminyl radicals **1**−**3** were generated, and **1** was isolated as radical crystals. The hfc constants of **1**−**3** were determined by ESR spectra. The spin density distribution in **1a** was calculated by ab initio MO calculations. The calculated hfc constants were in good agreement with the experimental values. Single-crystal X-ray crystallographic analysis was performed for **1c**, showing an approximately planar π-framework. The magnetic measurements of the isolated four radicals were performed. Two radicals showed ferromagnetic interactions and analyses with the one-dimensional regular Heisenberg model gave $2J/k_B = 5.8$ and 8.6 K. The other two radicals showed antiferromagnetic interactions. One of them showed a strong antiferromagnetic interaction ($2J/k_B = -1360$ K), and this magnetic behavior was well explained in terms of the X-ray crystallographic results.

Experimental Section

ESR spectra were obtained on a Bruker ESR 300 or JEOL TE 300 spectrometer. The hfc constants and g values were determined by a previously reported method.[13] SQUID measurements were carried out on a Quantum Design MPMS2 SQUID magnetometer using polycrystalline samples in the temperature range 1.8−300 K. The diamagnetic contribution was estimated using Pascal's constants. Column chromatography was carried out on alumina (Merck, aluminum oxide 90).

The preparations of 2,4,6-triphenylaniline, 2,4,6-tris(4-chlorophenyl)aniline, 2,6-diphenyl-4-acetylaniline, and 2,6-diphenyl-4-(ethoxycarbonyl)aniline are described in previous reports.[10,13] 2,4,6-Tris(phenyl-d_5)aniline was prepared from tribromoaniline and phenyl-d_5-boronic acid according to the same procedure as for the corresponding nondeuterio compound.[13,19] Bis(2-benzothiazolyl) and bis(2-pyrimidyl) disulfides were prepared by treating the corresponding sodium salts of mer-

(18) Bonner, J. C.; Fisher, M. E. *Phys. Rev.* **1968**, *165*, 647.

(19) Miura, Y.; Oka, H.; Momoki, M. *Synthesis* **1995**, 1419−1422.

Table 4. UV−Vis Spectra of 1−3 in Benzene

radical	λ_{max}, nm (ϵ, L mol^{-1} cm^{-1})
1a	342 (11800), 383 (16900), 394 (16800), 533 (1880, sh), 643 (8540)
1b	355 (18700, sh), 396 (27200), 533 (2870, sh), 656 (12300)
1c	332 (9780), 381 (20100), 396 (20800), 430 (8670, sh), 556 (3330, sh), 656 (8750)
1d	325 (9190), 388 (18900), 558 (3990, sh), 653 (8060)
2[a]	535 (sh), 620
3a[a]	536, 612
3b[a]	543, 619

[a] Because the radicals are not isolated, only λ_{max} values are shown.

captans with I_2 in ethanol. 2-Benzothiazolesulfenyl, 2-benzoxazolesulfenyl, and 2-pyrimidesulfenyl chlorides were prepared by bubbling Cl_2 into a solution of the corresponding bis(2-benzothiazolyl) or bis(2-pyrimidyl) disulfide (3.0−3.8 mmol) or 2-mercaptobenzoxazole (4.8 mmol) in CH_2Cl_2 (20 mL) at room temperature for ca. 0.5−2 min until the solution turned reddish yellow.[20] Then, N_2 was bubbled to remove the excess of Cl_2 in the sulfenyl chloride solution.

General Procedure for Preparation of 4. To a stirred solution of 4.00 mmol of an aniline and 3.8 mL of Et_3N in 200 mL of dry ether was added a solution of 2-benzothiazolesulfenyl chloride, prepared from 1.00 g (3.0 mmol) of bis(2-benzothiazolyl) disulfide, and the resulting mixture was stirred for 2 h at 0 °C. After filtration, the filtrate was evaporated under reduced pressure, and the residue was column chromatographed on alumina at 0 °C with 1:3 hexane−benzene (**4a**,**d**), 2:3 hexane−benzene (**4b**), or 1:5 ethyl acetate−hexane, giving **4a** in 42% yield, **4b** in 30% yield, **4c** in 68% yield, and **4d** in 56% yield. The products contained considerable amounts of **1**. The crude products were used in the following reaction without further purification. The deuterated compound **4a-***d* was prepared from 2,4,6-tris(phenyl-d_5)aniline and 2-benzothiazolesulfenyl chloride in the same manner as for **4a**.

General Procedure for Preparation of 5. To a stirred solution of 3.12 mmol of 2,4,6-triphenylaniline and 3.0 mL of Et_3N in 150 mL of dry ether was added a solution of 2-benzoxazolesulfenyl chloride, prepared from 0.72 g (4.8 mmol) of 2-mercaptobenzoxazole, and the resulting mixture was stirred for 2 h at 0 °C. After filtration, filtrate was evaporated under reduced pressure, and the residue was column chromatographed on alumina at 0 °C with 1:1 hexane−benzene. After evaporation under reduced pressure, the residue obtained was used in the next reaction without purification. The deuterated compound **5-***d* was prepared from 2,4,6-tris(phenyl-d_5)aniline and 2-benzoxazolesulfenyl chloride in the same manner as for **5**.

General Procedure for Preparation of 6. To a stirred solution of 5.0 mmol of aniline and 3.5 mL of Et_3N in 200 mL of dry ether was added a solution of 2-pyrimidinesulfenyl chloride, prepared from 0.83 g (3.75 mmol) of bis(2-pyrimidyl) disulfide, and the resulting mixture was stirred for 2 h at 0 °C. After filtration, filtrate was evaporated under reduced pressure, and the residue was column chromatographed on alumina at 0 °C with 1:5 ethyl acetate−hexane (**6a**) or 2:3 hexane−benzene (**6b**), giving **6a** in 43% yield and **6b** in 65% yield. Recrystallization from hexanes−ethyl acetate gave colorless prisms. The deuterated compound **6a-***d* was prepared from 2,4,6-tris(phenyl-d_5)aniline and 2-pyrimidinesulfenyl chloride in the same manner as for **6a**.

***N*-(2-Pyrimidylthio)-2,4,6-triphenylaniline (6a):** colorless prisms, mp 71−73 °C; IR (KBr) 3340 cm^{-1} (NH); ^{1}H NMR ($CDCl_3$) δ 5.84 (s, 1H), 6.77 (t, J = 4.9 Hz, 1 H), 7.27−7.44 (m, 9 H), 7.45 (s, 2H), 7.58 (d, J = 8.3 Hz, 4 H), 7.60 (d, J = 8.3 Hz, 2H), 8.24 (d, J = 4.9 Hz, 2 H). Anal. Calcd for $C_{28}H_{21}N_3S$: C, 77.93; H, 4.90; N, 9.74. Found: C, 78.30; H, 4.81; N, 9.77.

***N*-(2-Pyrimidylthio)-2,4,6-tris(4-chlorophenyl)-aniline (6b):** colorless prisms, mp 143.5−145 °C; IR (KBr) 3340 cm^{-1} (NH); ^{1}H NMR ($CDCl_3$) δ 5.68 (s, 1H), 6.86 (t, J = 4.9 Hz, 1 H), 7.36 (s, 2H), 7.37 (d, J = 8.3 Hz, 2H), 7.40 (d, J = 8.3 Hz, 4 H), 7.49 (d, J = 8.3 Hz, 4H), 7.50 (d, J = 8.3 Hz, 2 H), 8.29 (d, J = 4.9 Hz, 2 H). Anal. Calcd for $C_{28}H_{18}Cl_3N_3S$: C, 62.87; H, 3.39; N, 7.86. Found: C, 63.11; H, 3.66; N, 7.62.

***N*-(2-Pyrimidylthio)-2,4,6-tris(phenyl-d_5)aniline (6a-*d*):** colorless prisms, mp 70−72 °C; IR (KBr) 3340 cm^{-1} (NH); ^{1}H NMR ($CDCl_3$) δ 5.84 (s, 1H), 6.77 (t, J = 4.9 Hz, 1 H), 7.45 (s, 2H), 8.24 (d, J = 4.9 Hz, 2 H).

General Procedure for Isolation of 1. To a vigorously stirred solution of 300 mg of **4** in 20 mL of benzene was added 9.0 g of PbO_2 over 2 min in several portions, and stirring was continued for an additional 1 min. After filtration, the benzene was removed by freeze-drying, and the residue was crystallized from ethanol−ethyl acetate (**1a**,**b**,**d**) or ethanol (**1c**).

***N*-[(2-Benzothiazolyl)thio]-2,4,6-triphenylphenylaminyl (1a):** dark green needles; mp 151−153 °C; yield 22%. Anal. Calcd for $C_{31}H_{21}N_2S_2$: C, 76.67; H, 4.36; N, 5.77. Found: C, 76.39; H, 4.58; N, 5.58.

***N*-[(2-Benzothiazolyl)thio]-2,4,6-tris(4-chlorophenyl)-phenylaminyl (1b):** dark green plates; mp 154−156 °C; yield 18%. Anal. Calcd for $C_{31}H_{18}Cl_3N_2S_2$: C, 63.22; H, 3.08; N, 4.76. Found: C, 63.49; H, 3.22; N, 4.53.

***N*-[(2-Benzothiazolyl)thio]-4-acetyl-2,6-diphenylphenylaminyl (1c):** dark blue plates; mp 133−135 °C; yield 15%. Anal. Calcd for $C_{27}H_{19}N_2OS_2$: C, 71.81; H, 4.24; N, 6.20. Found: C, 71.58; H, 4.30; N, 5.90.

***N*-[(2-Benzothiazolyl)thio]-4-(ethoxycarbonyl)-2,6-bis-(4-chlorophenyl)phenyl aminyl (1d):** dark blue needles; mp 163−165 °C; yield 11%. Anal. Calcd for $C_{28}H_{19}Cl_2N_2O_2S_2$: C, 61.09; H, 3.48; N, 5.09. Found: C, 60.96; H, 3.57; N, 4.92.

UV−Vis Spectral Data. The The UV−Vis spectral data for **1**−**3** are summarized in Table 4.

X-ray Crystallographic Analysis for 1c.[21] A black platelet crystal of $C_{27}H_{19}N_2OS_2$ (451.58) having approximate dimensions of 0.5 × 0.5 × 0.1 mm was mounted on a glass fiber. All measurements were made on a Rigaku RAXIS-RAPID Imaging Plate diffractometer with graphite monochromated Mo Kα radiation (λ = 0.71069 Å): monoclinic space group $P2_1/c$, a = 12.3168(4), b = 11.4207(5), c = 16.1587(6) Å, β = 103.645(2)°, V = 2208.8(1) Å^3, Z = 4, and D_c = 1.358 g cm^{-3}. The data were collected at 23 ± 1 °C to a maximum 2θ value of 55.0°. A total of 44 images, corresponding to 220.0° oscillation angles, were collected with 2 different goniometer settings. Exposure time was 7.50 min/deg. The camera radius was 127.40 mm. Readout was performed in the 0.150 mm pixel mode. Data were processed by the PROCESS-AUTO program package. Of 20997 reflections measured 5055 were unique (R_{ini} = 0.045), 2615 of which were considered as observed ($I > 3.10\sigma(I)$).

The structure was solved by direct methods and expanded using Fourier techniques.[22] The non-hydrogen atoms were refined anisotropically. Hydrogen atoms were placed in the fixed position and not refined. The final cycle of full matrix least-squares refinement was based on 2615 observed reflections and 290 variable parameters and converged with unweighted and weighted agreement factors of R = 0.071 and R_w = 0.120. GOF = 1.91.

Acknowledgment. This work was in part financially supported by Grant-in-Aids for Scientific Research on Priority Area (A) (No.10146246 and 11133253) from the Ministry of Education, Science, Sports and Culture of Japan.

Supporting Information Available: Tables of X-ray structural data for compound **1c** and ESR spectra of **1a**,**b**,**d**, **2**, **2-***d*, **3a**,**b**, and **3a-***d*. This material is available free of charge via the Internet at http://pubs.acs.org.

JO000901Q

(20) Long time bubbling of Cl_2 yielded unsoluble materials.

(21) The crystallograhpic computing was done by the TEXSAN structure analysis software.

(22) SIR92: Altomare, A.; Burla, M. C.; Camalli, M.; Cascarano, M.; Giacovazzo, C.; Guagliardi, A.; Polidori, G. *J. Appl. Crystallogr.* **1994**, *27*, 435.